Finite Element Modelling Of Composite Steel-Concrete Beams with External Pressurising

K. Chandramohanmouli, N. Harish Kumar
PG Student, Assistant Professor
Dhirajlal Gandhi College of Technology, Salem,

ABSTRACT: In this paper, a nonlinear finite-element analyses have been carried out to investigate the behaviour up to failure of simply supported composite steel-concrete beams with external prestressing, in which a concrete slab is connected together with steel I-beam by means of headed stud shear connectors, subjected to symmetrically static loading. ANSYS computer program (version 12.0) has been used to analyze the three dimensional model. This covers: load deflection behavior, strain in concrete, strain in steel beam and failure modes. The nonlinear material and geometrical analysis based on Incremental-Iterative load method, is adopted. Three models have been analyzed to verify its capability and efficiency. The results obtained by finite element solutions have shown good agreement with experimental results.

1. INTRODUCTION

The use of external prestressing as a means of strengthening or rehabilitating existing bridges has been used in many countries since the 1950s. It has been found to provide an efficient and economical solution for a wide range of bridge types and conditions. The technique is growing in popularity because of the speed of installation and the minimal disruption to traffic flow. The principle prestressing, is the application of an axial load combined with a hogging bending moment to increase the flexural capacity of a beam and improve the cracking performance. It can also have a beneficial effect on shear capacity (Dally, 1997).

Composite steel - concrete beams prestressed with high strength external tendons have demonstrated many advantages as compared with plain composite beams: Increase in ultimate moment capacity of structure, Enlarge the range of elastic behavior before yielding for the structure with the introduction of internal stresses. The stresses can then oppose the moment generated by the loading. The amount of structural steel used in construction, based on yield

strength alone, can be significantly reduced by the use of high-strength tendons, thereby reducing the cost of construction. A composite beam can be prestressed, using a jack, by the tensioning high-strength tendons connected at both ends to brackets or anchorages that are fixed to the composite beam. Prestressing a composite beam can introduce internal stresses into the member cross sections that can be defined for different purposes. Such induced stresses can then counteract the external loads applied on the structure. Prestressing can be carried out for simple-span or continuous-span composite beams. In the positive moment region, the steel beam is usually prestressed before the concrete is cast because the negative moment induced by prestressing may be used to counteract the positive moments caused by the concrete's self weight. In the negative moment region, the steel beam and concrete deck can also be prestressed either separately or jointly along the top flange before or after casting of the deck Saadatmanesh (1989).

Previous research has been done on prestressed steel and concrete composite beams with external tendons such as by Saadatamanesh(1989) , by Saadatamanesh(1989) and Ayyub(1990) , Nie J.(2007) , Zona A.(2009) and Chen Sh.(2009) In this paper, a 3D nonlinear finite element model using the finite element program ANSYS version 12.0 has been developed to account for the non-linear behavior in composite beams prestressed with external tendons. To examine the model verification was done using the experimental results of Saadatmanesh et al. Saadatmanesh (1989)and Ayyub et al. Ayyub B (1990).Using those models, numerical analysis was performed and compared with the experimental results.

2. FINITE ELEMENT MODEL

The ANSYS computer program is utilized for analyzing structural components encountered throughout the current study. Finite element representation and corresponding elements designation in ANSYS used in this study are discussed,

2.1 FINITE ELEMENT MODEL OF CONCRETE

The finite element idealization of concrete should be able to represent the concrete cracking, crushing, the interaction between concrete and reinforcement and the capability of concrete to transfer shear after cracking by aggregate interlock. In order to investigate the failure in concrete for prestressed composite steel-concrete beams, three dimensional elements are to be used. In the current study, three-dimensional brick element with 8 nodes is used to model the concrete (SOLID65 in ANSYS). The element is defined by eight

nodes having three degrees of freedom at each node: translations of the nodes in x, y, and z-directions. The geometry, node locations, and the coordinate system for this element are shown in Figure 1.

```
ET,MATID,SOLID65
R,MATID,0,0,0,0,0,0
RMORE,0,0,0,0,0

MP,EX,MATID,29250
MP,PRXY,MATID,0.2
MPTEMP,MATID,0

TB,CONCR,MATID,1,9
TBTEMP,22
TBDATA,1,0.3,0.8,1.5,25

TB,MISO,MATID,1,35,0
TBTEMP,22
TBPT,,0.0001,2.925
TBPT,,0.0002,5.7
TBPT,,0.0003,8.325
TBPT,,0.0004,10.8
TBPT,,0.0005,13.125
TBPT,,0.0006,15.3
TBPT,,0.0007,17.325
TBPT,,0.0008,19.2
TBPT,,0.0009,20.925
TBPT,,0.001,22.5
TBPT,,0.0011,23.925
TBPT,,0.0012,25.2
TBPT,,0.0013,26.325
TBPT,,0.0014,27.3
TBPT,,0.0015,28.125
TBPT,,0.0016,28.8
TBPT,,0.0017,29.325
TBPT,,0.0018,29.7
TBPT,,0.0019,29.925
TBPT,,0.002,30
TBPT,,0.0021,30
TBPT,,0.0022,30
TBPT,,0.0023,30
TBPT,,0.0024,30
TBPT,,0.0025,30
TBPT,,0.0026,30
```

TBPT,,0.0027,30
TBPT,,0.0028,30
TBPT,,0.0029,30
TBPT,,0.003,30
TBPT,,0.0031,30
TBPT,,0.0032,30
TBPT,,0.0033,30
TBPT,,0.0034,30
TBPT,,0.0035,30

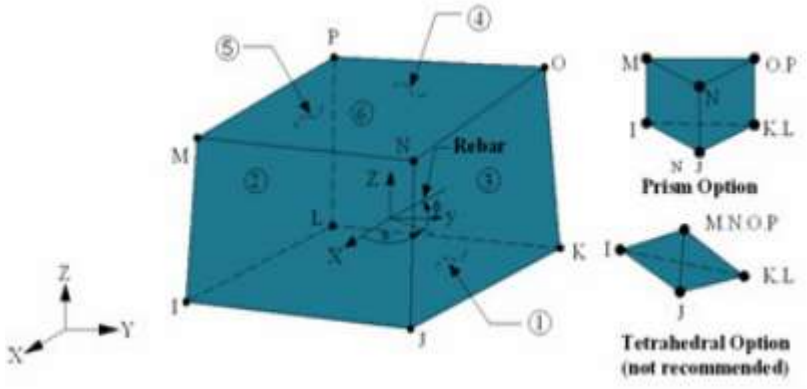

2.2 FINITE ELEMENT MODEL OF STEEL BEAM

To represent the steel beam in finite element, 4-node shell element is needed with three translations in x, y and z in each node to achieve the compatibility condition with translation in x, y and z in adjacent brick element to it. For this purpose, three-dimensional 4-node shell element, which is represented as (SHELL43 in ANSYS) is used, regardless of the rotations in each nodes. The element has plasticity, creep, stress stiffening, large deflection, and large strain capabilities. The geometry, node locations, and the coordinate system for this element are shown in Figure 2.

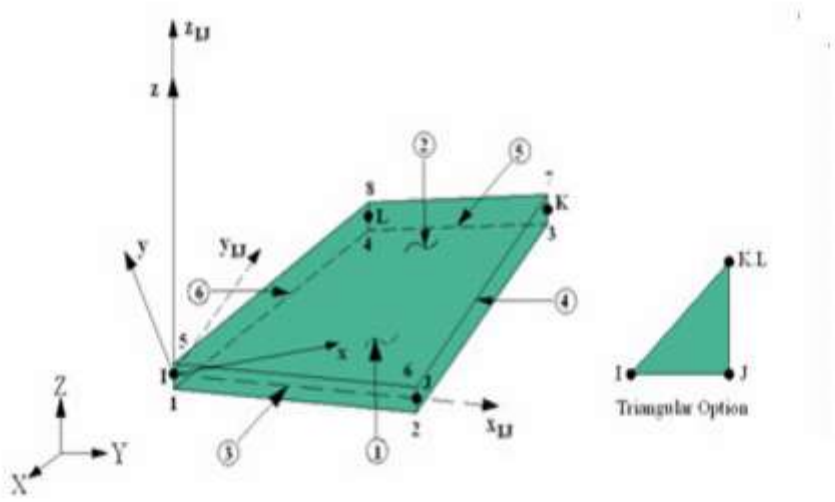

1.3 FINITE ELEMENT MODEL OF REINFORCEMENT

To model steel reinforcement in finite element. Three techniques exist these are discrete, embedded, and smeared. The discrete model (LINK8) is used in this study. The LINK8 is a spar (or truss) element. This element can be used to model trusses, sagging cables, links, springs, etc. The 3-D spar element is a uniaxial tension-compression element with three degrees of freedom at each node: translations of the nodes in x, y, and z-directions. No bending of the element is considered. The geometry, node locations, and the coordinate system for this element are shown in Figure 3.

ET,MATID,LINK180
MPDATA,EX,MATID,,2e5
MPDATA,PRXY,MATID,,0.3
TB,BISO,MATID,1,2
TBDATA,,460,2100
R,MATID,12,,0

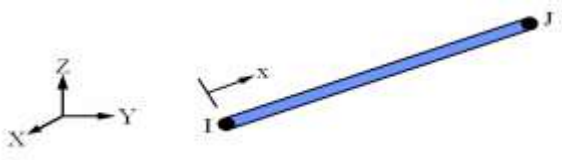

1.4 FINITE ELEMENT MODEL OF EXTERNAL PRESTRESSED TENDON

In the present study the prestressing stress was taken as the initial value and equal to the effective stress .It appears in the analysis as initial strain in link element. Link8 is used to represent the external cable. Since the cable is located outside the steel section and the prestressing force is transferred to composite

beam through end anchorages and stiffeners, the cable is connected to beam only at the anchorage or stiffeners.

1.5 FINITE ELEMENT MODEL OF STEEL PLATES

Steel plates are added at the loading location to avoid stress concentration problems. This provides a more even stress distribution over the load area. The solid element (SOLID45 in program) was used for the steel plates. The element is used for the 3-D modeling of solid structures. The element is defined by eight nodes having three degrees of freedom at each node: translations in the nodal x, y, and z directions as shown in Figure (4).

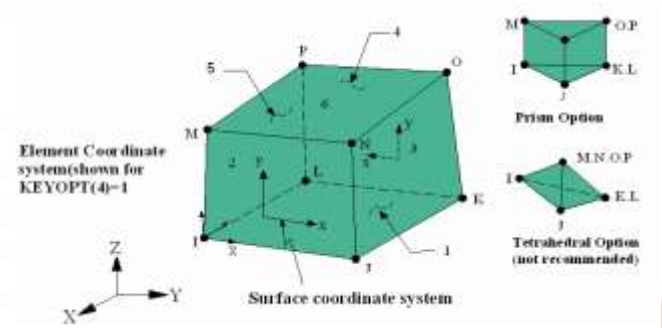

1.6 FINITE ELEMENT MODEL OF INTERFACE SURFACE

A three-dimensional nonlinear surface-to-surface "contact-pair" element (CONTA-173& TARGE170) was used to model the nonlinear behavior of the interface surface between concrete and steel beam. The contact-pair consists of the contact between two boundaries, one of the boundaries represents contact, slid and deformable surface taken as contact surface (CONTA-173 in ANSYS) and the other represents rigid surface taken as a target surface (TARGE-170 in ANSYS). Figure 5 shows the geometry of (CONTA173& TARGE170).

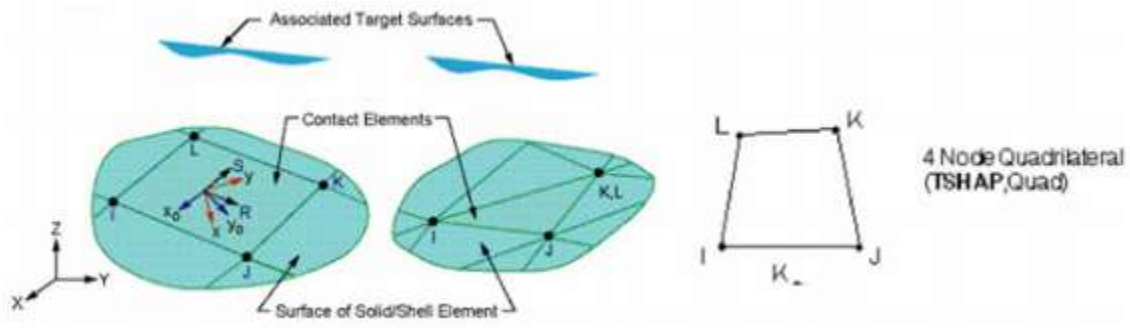

3. MATERIAL MODELLING

In this study, the main components of prestressed composite section: concrete slab, steel beam, tendons, contact surface and shear connection are modeled with relevant ANSYS elements that are explained in sequel. A three dimensional element was used to representation the structure.

3.1 MODELING OF CONCRETE

The concrete is assumed to be homogeneous and initially isotropic. The adopted stress-strain relation is based on work done by Desayi and Krishnan [8]

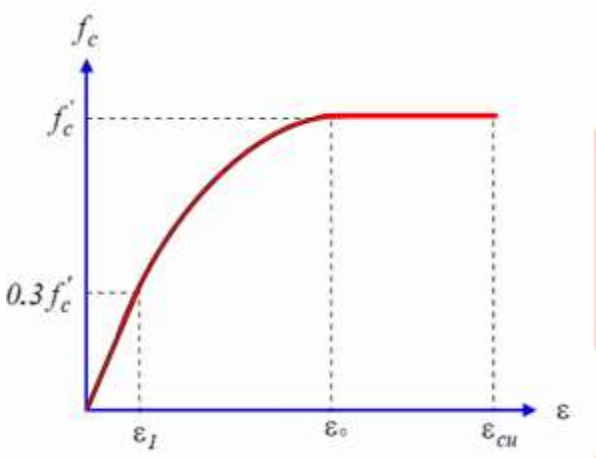

Compressive uniaxial stress-strain relationship for concrete model was obtained by using the following equations to compute the multilinear isotropic stress-strain curve for the concrete.

$$f_c = \varepsilon E_c \qquad \text{for} \quad 0 \le \varepsilon \le \varepsilon_1 \qquad \text{.....(1)}$$

$$f_c = \frac{\varepsilon E_c}{1 + \left(\frac{\varepsilon}{\varepsilon_0}\right)^2} \qquad \text{for} \quad \varepsilon_1 \le \varepsilon \le \varepsilon_0 \qquad \text{..... (2)}$$

$$f_c = f_c' \qquad \text{for} \quad \varepsilon_0 \le \varepsilon \le \varepsilon_{cu} \qquad \text{..... (3)}$$

$$\varepsilon_1 = \frac{0.3 f_c'}{E_c} \qquad \text{(Hooke's law)} \qquad \text{..... (4)}$$

$$\varepsilon_0 = \frac{2 f_c'}{E_c} \qquad \text{..... (5)}$$

Where:

ε_1 =strain corresponding to ($0.3f_c'$), ε_0 =strain at peck point, ε_{cu}= ultimate compressive strain.

3.2 MODELING OF STEEL BEAM

In contrast to concrete, the mechanical properties of steel are well known, and it is a much simpler material to be represented. The strain-stress behavior can be assumed to be identical in tension and compression. The bilinear stress-strain relationship indicated is used in this study [9] . In the present work, the strain hardening modulus (Et) is assumed to be (0.03 Es). This value is selected to avoid convergence problems during iteration.

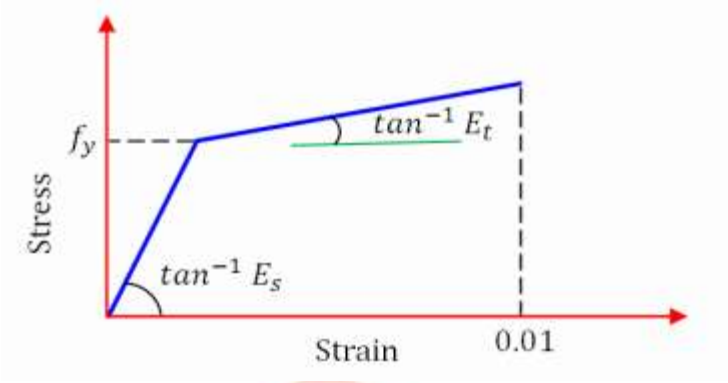

3.3 MODELING OF REINFORCEMENT AND PRESTRESSING BARS

Since the ordinary steel bars and prestressing cable are slender, they can be assumed to transmit axial force only. Modeling of ordinary steel and prestressed steel in finite element is much simpler. The stress-strain relationship for ordinary reinforcing steel and prestressing tendons can be represented as shown in Figure 8.

3.4 SHEAR FRICTION AND CONTACT MODELING

In the basic Coulomb friction model, the two contacting surfaces can carry shearing stress up to a certain magnitude across their interface before they start sliding relative to each other; this state is known as contact (sticking). Once the shearing stress is exceeded, the two surfaces will slide relative to each other and this state is known as (sliding). In the present work, coefficient of friction with (μ=0.7) has been used.

3.5 MODELING OF SHEAR CONNECTOR

The normal forces transmitted by the axial forces in the reinforcing bars are modeled by using a link element (LINK8 in ANSYS), while, the shear forces that are transmitted by shearing and flexure of the reinforcing bars are modeled by using a nonlinear spring element (COMBIN39 in ANSYS). The equation used to modeling the behavior of shear connector is:

$$F_{fl} = F_{flu}\left(1 - \frac{1}{e^{QV_s}}\right)^{Q} .55B$$

4. ANALYTICAL MODEL

In this paper, prestressed composite steel-concrete beams are analyzed; the dimensions of the beams are illustrated in Figure 9 to Figure 11 .Three beams, VS-1, VS-2, and VS-3 were analyzed in this study are selected to investigate the behavior of externally prestressed composite steel-concrete beams, by develop a general analytical approach to predict the ultimate flexural response. The accuracy and validity of the finite element models is determined by ensuring that failure modes are correct, the ultimate load is reasonably predicted in comparison with the available experimental investigations. VS-1 is tested by Saadatmanesh et al. The beam is simply supported composite steel-concrete beam, having prestressing bars along the bottom flange and which is subjected to positive bending moment as shown in Figure 9. VS-2, and VS-3 were tested by Ayyub et al. VS-2 is simply supported consisted of a concrete slab, a steel beam, and two prestressing tendons as shown in Figure 10 . The prestressing bars were anchored at the two ends of the beam 30 mm above the bottom (tension) flange and were extended on both sides of the web along the full length of the beam.

Beam VS-3 is similar to beam VS-2 and was prestressed with draped tendon profile, as shown in Figure 11. The tendons were anchored at both ends of the centroid axis of the composite section, 32 mm below the top flange and were positioned between the loading points 30 mm above the bottom flange. A summary of the materials properties of the selected beams are listed in Table 1.

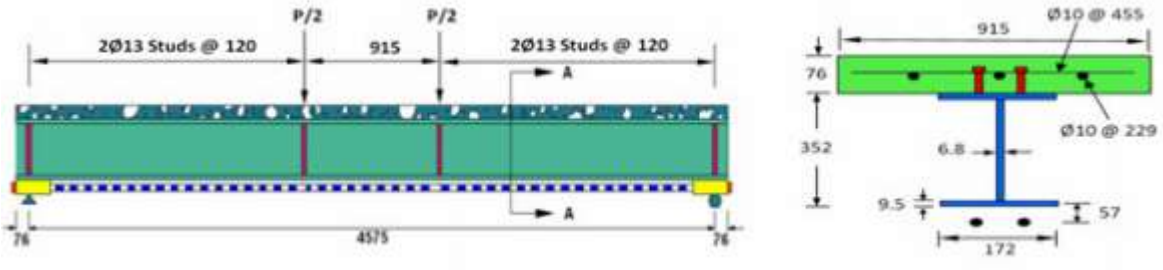

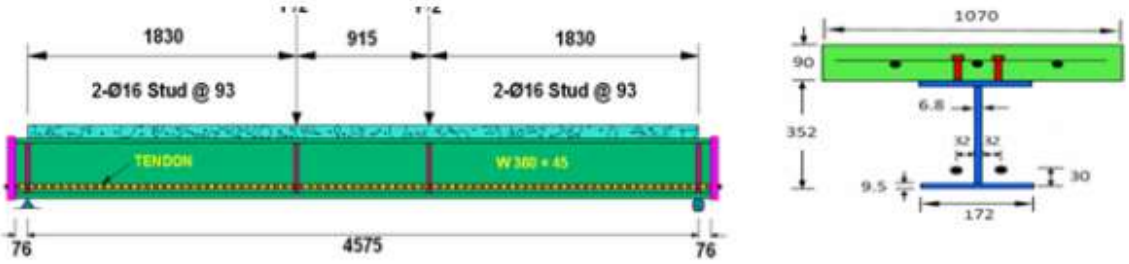

Figure 10: Details of Beam (VS-2)

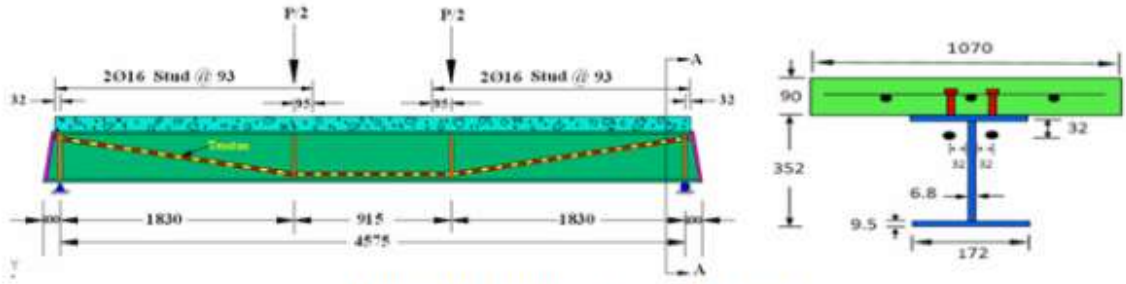

Figure 11: Details of Beam (VS-3)

Table 1: Summary of Material properties

Beam	Prestressing Tendons				f'_c(MPa)	fy (MPa)
	Position*	fpe (MPa)	Ap(mm^2)	fpy (MPa)		
VS-1	57	544	180	910	33.4	367
VS-2	30	741	180	915	40	411.6
VS-3	30	1046	139.5	1620	40	411.6

5. ANALYSIS RESULTS

5.1 LOAD-DEFLECTION CURVE

The load-midspan deflection curves of the prestressed composite steel-concrete beams obtained from the finite element analysis was compared with corresponding experimental data as shown in figures from (12) to (14) . In general, it can be noted from the loaddeflection curves that the finite element analyses are agree well with the experimental results throughout the entire range of behavior.

5.2 ULTIMATE LOAD AT FAILURE

Table 2 shows the comparison between the ultimate loads of the experimental (tested) beams, (Pu)EXP., and the final loads from the finite element models, (Pu)FEM. The final loads for the finite element models are the last applied load steps before the solution starts to diverge due to numerous cracks and large deflections.

The numerical model predicts ultimate loads of (656.7 kN), (723 kN) and (769.9kN) for beams (VS-1), (VS-2) and (VS-3) respectively and captures well the nonlinear loaddeflection response of the beams up to failure as mentioned before.

In comparison with the experimental values, the numerical models show (2.7%), (1.68%) and (0.66%) increase in ultimate loads for the beams (VS-1), (VS-2) and (VS-3) respectively. As shown in Table (2), the ultimate loads obtained from numerical model agree well with the corresponding values of the experimental (tested) beams.

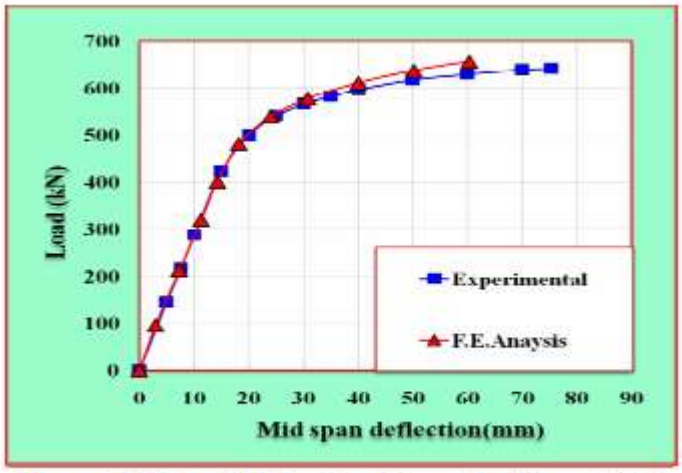

Figure 12: Load-Deflection Curve for Beam VS-1

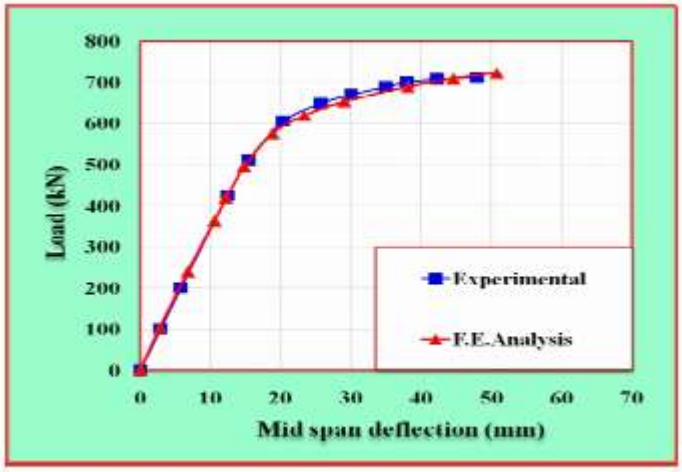

Figure 13: Load-Deflection Curve for Beam VS-2

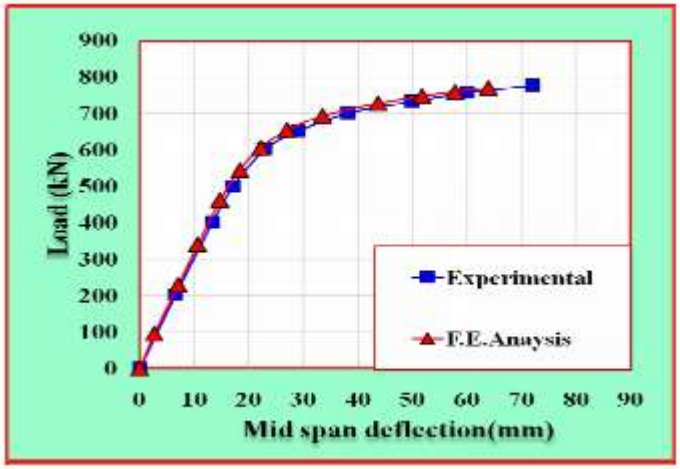

Table 2: Ultimate loads from experimental test and Finite element analysis

Analytic and test beam	Ultimate load (kN)		$\frac{(Pu)_{FEM}}{(Pu)_{EXP}}$	Difference Ratio
	$(Pu)_{FEM.}$	$(Pu)_{EXP.}$		
VS-1	656.7	641	1.02	2.4%
VS-2	723	711	1.01	1.68%
VS-3	769.9	775	0.993	0.66%

5.3 DEFLECTED SHAPE

Deflections (Vertical displacements) were measured at mid-span at the center of the bottom face of the beams, in y-direction (Uy). A deflected shape for two load steps, camber arising from the effect of prestressing force in the external tendon; and deflected shape due to externally applied loads for all beams are shown in Figures below:

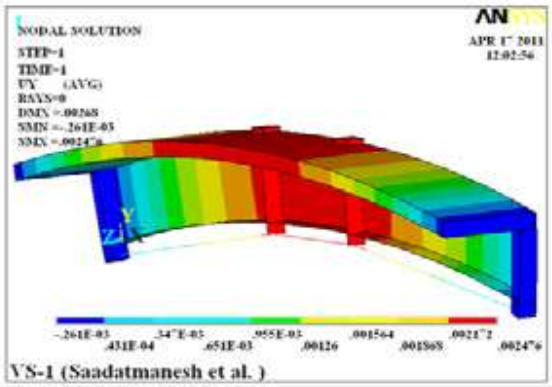

Figure 15: Initial Camber of the Beam VS-1 with no Applied Concentrated Load

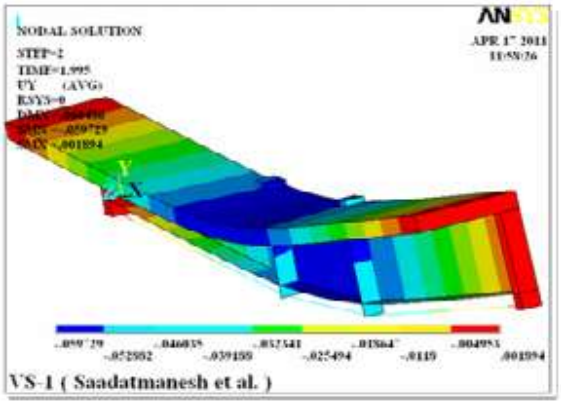

Figure 16: Deflected Shape for Beam VS-1 at Load = 656.7 kN

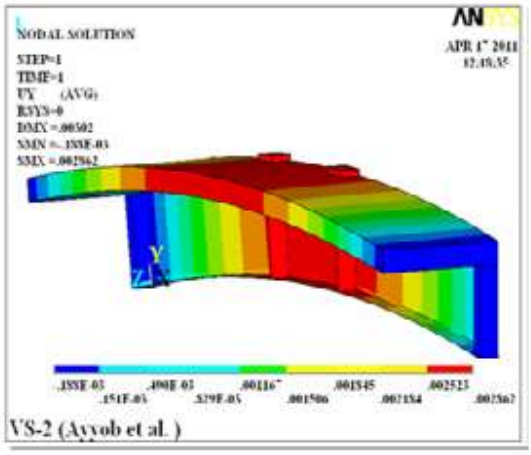

Figure 17: Initial Camber of the Beam VS-2 with no Applied Concentrated Load

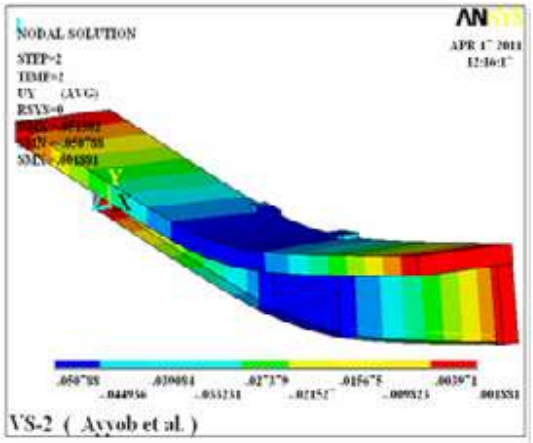

Figure 18: Deflected Shape for Beam VS-2 at Load = 723 kN

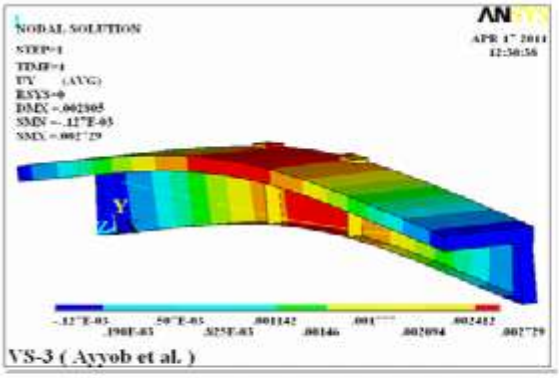

Figure 19: Initial Camber of the Beam VS-3 with no Applied Concentrated Load

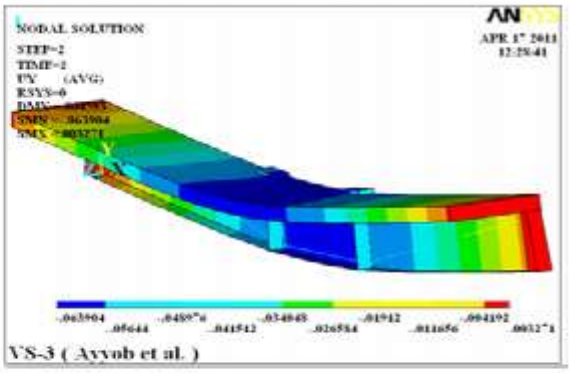

Figure 20: Deflected Shape for Beam VS-3 at Load=769.9kN

5.4 LOAD-STRAIN CURVES

Figure 21 shows the load versus extreme compression fiber strain response of the concrete slab observed from experimental and analytical study (computer program) of (VS-1) beam. It is shown that the analytical compressive strains and corresponding experimental strains are very close throughout the loading up to the yielding then the analytical strain become slightly higher than the experimental strain up to ultimate load.

Figure 22 shows comparison between experimental results and numerical results that are obtained by ANSYS computer program for load versus strain in the prestressed bars. The strain in the bar was recorded up to yielding. The curves were offset from the origin of the coordinate system by the initial prestressing strains. This Figure shows the increase in strain in the prestressing tendons with loading. Both the tendons were prestrained to an initial strain of 2700 micro-strain reaching a load of 98 kN in each of the tendons.

Figures 23 and 24 shows the load versus strain curves for the bottom and top steel flange observed from experimental and analytical study. All the curves were offset from the origin by the strain induced during the initial prestressing. The strain in the bottom flange was recorded up to yielding. Higher strain values were recorded in the bottom flange than the top flange.

Both top and bottom steel flanges curves started incompression and moved towards the right side of the curve as the external load started to neutralize their initial precompression due to prestressing. At a load of about 98 kN, the initial precompression was reduced to almost zero as the load was increased. It was observed that the behavior still linear up to a load of 455 kN where the bottom flange of steel beam is yielded.

Figures from 25 to 28 shows comparison between experimental results and numerical results for load versus strain in extreme fiber of the top and bottom concrete slab, top and bottom flange of steel beam respectively for (VS-2) beam. It is shown that the analytical compressive strains and corresponding experimental strains are very close throughout the loading up to ultimate load. Higher strain values were recorded in the bottom flange than the top flange. Figure 29 shows the load versus extreme compression fiber strain response of the concrete slab of (VS-3) beam. It is

shown that the analytical compressive strains and corresponding experimental strains are very close. In Figures 30 and 32, shows the midspan load versus strain for bottom concrete, top, and bottom flange of the (VS-3) beam. Higher strain values were recorded in the bottom flange than the top flange.

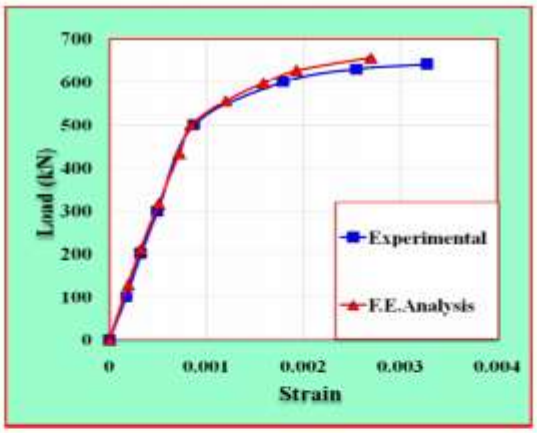

Figure 21: Load-strain curve for extreme compression concrete fiber of vs-1

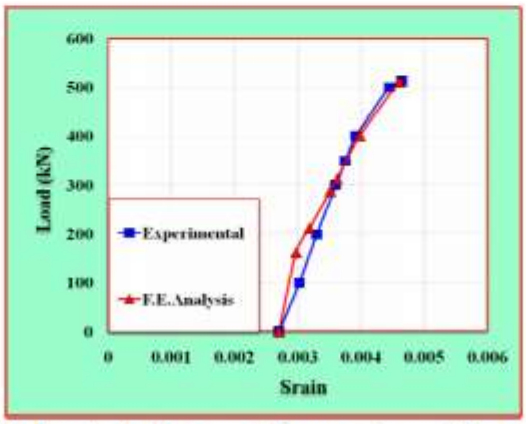

Figure 22: Load-strain curve for prestressed bars for VS-1

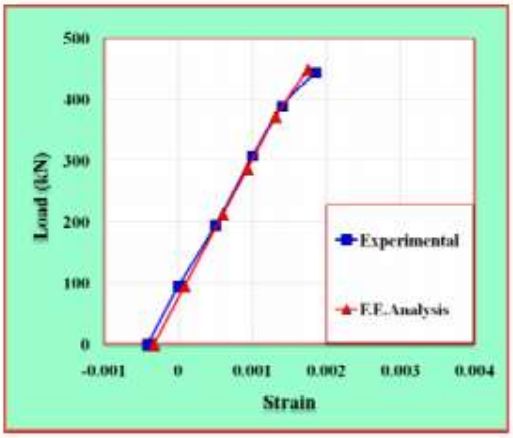

Figure 23: Load-strain curve for bottom flange for VS-1

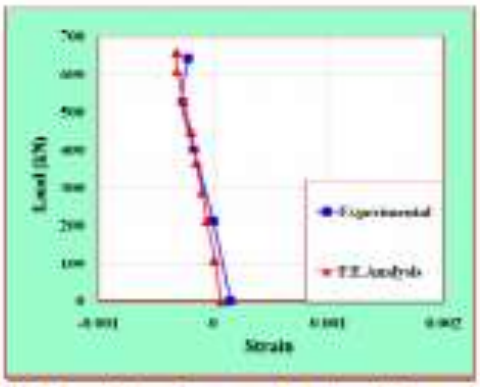

Figure 24: Load-strain curve for top flange for VS-1

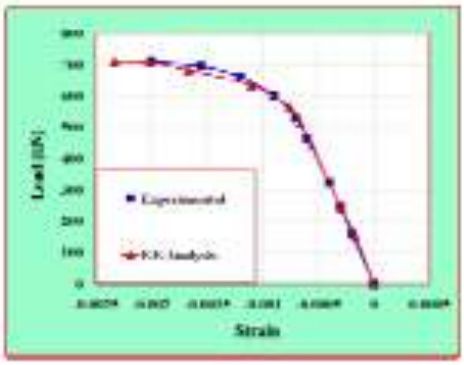

Figure 25: Load-strain curve for extreme compression concrete fiber of VS-2.

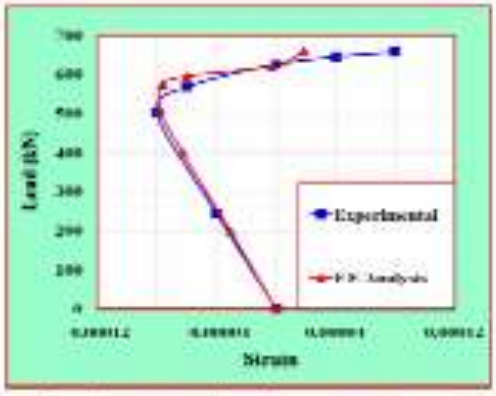

Figure 26: Load-strain curve for bottom concrete fiber for VS-2.

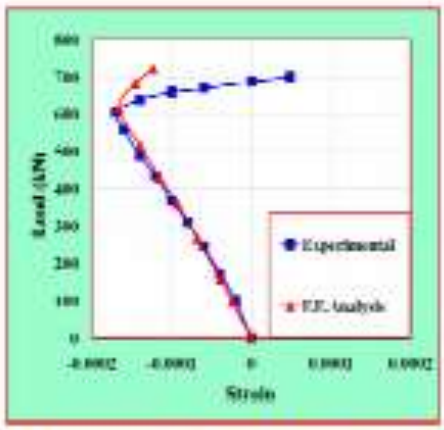

Figure 27: Load-strain curve for top flange for VS-2

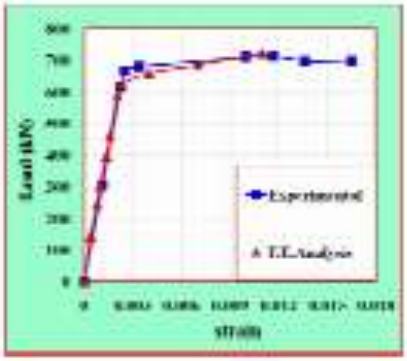

Figure 28: Load-strain curve for bottom flange for VS-2

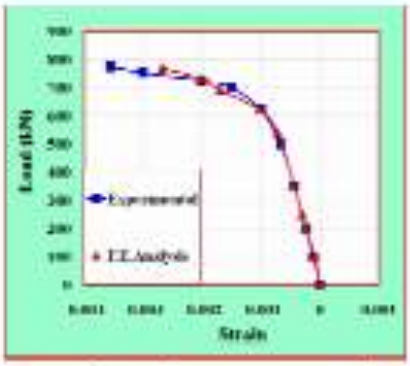

Figure 29: Load-strain curve for extreme compression concrete fiber for VS-3

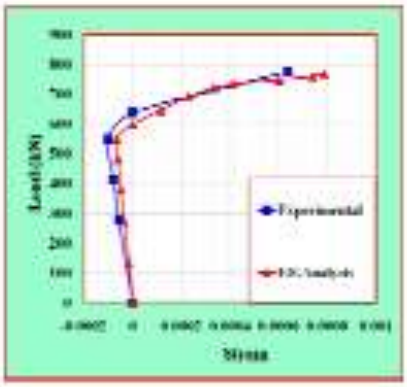

Figure 30: Load-strain curve for bottom concrete for VS-3

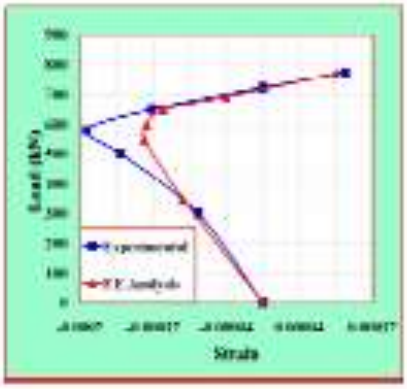

Figure 31: Load-strain curve for top flange for VS-3

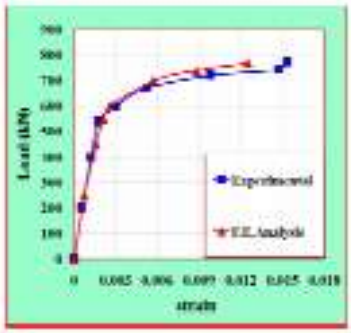

Figure 32: Load-strain curve for bottom flange for VS-3

5.5 CONCLUSIONS

The finite element model used in the present work is able to simulate the behavior of prestressed composite steel-concrete beams. The analytical tests carried out for the different cases studied (straight and draped) indicated that the load-deflection behavior and the ultimate loads are in good agreement with the published experimental results. The maximum difference between the predicted numerical ultimate load to the experimental ultimate load for all cases has value of (2.4%) for prestressed composite steel-concrete beams. These results reveal the accuracy and efficiency of the developed computer program (ANSYS 12) in predicting the behavior and ultimate load of prestressed composite steel-concrete beams. The results also showed the load strain behavior in concrete slab and steel beam are in good agreement with the experimental results. 6 .

REFERENCES

1. Daly F., Witarnawan W., (1997), Strengthening of bridges using external posttensioning, Conference of eastern Asia society for transportation studies, Seoul, Korea.

2. Saadatmanesh H., Albrecht P., and Ayyub B., (1989), Guidelines for flexural design of prestressed composite beams, Journal of structural engineering, ASCE, 115(11), pp 2944-2961

3. Saadatmanesh H., Albrecht P., and Ayyub B., (1989), Experimental study of prestressed composite beams, ASCE, Journal of structural engineering, 115(9), pp 2348-2363.

4. Ayyub B., Sohn Y., and Saadatmanesh H., (1990), Prestressed composite girders under positive moment, ASCE, Journal of structural engineering, 116(11), pp 2931- 2951

5. Nie J., Cai C., Zhou T., and Li Y., (2007), 'Experimental and analytical study of prestressed steel-concrete composite beams considering slip effect,' ASCE, Journal of structural engineering, 133(4), pp 530-540.

6. Zona A., Ragni L., and Dall'Asta A., (2009), A simplified method for the analysis of externally prestressed steel-concrete composite beams, Journal of constructional steel research, 65, pp 308-313.

7. Chen Sh., Wang X., and Jia Y., (2009), 'A comparative study of continuous steelconcrete composite beams prestressed with external tendons: Experimental investigation, Journal of constructional steel research, 65, pp 1480-1489.

8. Desayi P., and Krishnan, S., (1964), Equation for the stress-strain curve of concrete, Journal of the American concrete institute, 61, pp 345- 350

9. European Committee for Standardisation (CEB), Eurocode 3, (1993), Design of steel structures, Part 1.1: General rules and rules for buildings, DD ENV, 1993-1-1, EC3.

10. Millard S., and Johnson R., (1984), Shear Transfer across cracks in reinforced concrete due to aggregate interlock and to dowel action, Magazine of concrete research, 36(126), pp 9-21.